Available online at www.sciencedirect.com

SciVerse ScienceDirect

Ceramics International 39 (2013) S227–S231

CERAMICS INTERNATIONAL

www.elsevier.com/locate/ceramint

Dielectric properties of strontium iron holmium niobate ceramics

K. Sanjoom[a,c], T. Tunkasiri[a,b], K. Pengpat[a,b], S. Eitssayeam[a,b], G. Rujijanagul[a,b,c,*]

[a]Department of Physics and Materials Science, Faculty of Science, Chiang Mai University, Chiang Mai 50200, Thailand
[b]Materials Science Research Center, Faculty of Science, Chiang Mai University, Chiang Mai 50200, Thailand
[c]Thailand Center of Excellence in Physics, Commission on Higher Education, 328 Sri Ayutthaya Road, Bangkok 10400, Thailand

Available online 16 October 2012

Abstract

Strontium iron holmium niobate ($Sr(Fe_{1-x}Ho_x)_{0.5}Nb_{0.5}O_3$) ceramics were synthesized via a solid-state reaction technique. The undoped ceramic showed an orthorhombic phase, but it transformed to a pseudocubic phase for higher Ho concentrations. A low solubility limit of Ho in SFN caused a formation of second phase for the $x=0.15$ ceramic. Dielectric behavior of undoped ceramic exhibited high dielectric constant over a wide temperature range. However, the doping shifted this region to a higher temperature. The doping also shifted the peak of dielectric loss to a higher temperature. Activation energy of dielectric relaxation increased with increasing Ho concentration. In addition, complex impedance analysis was applied to determine the behaviors of grain boundary and grain after doping.

Keywords: A. Powders: solid state reaction; B. Grain boundaries; C. Dielectric properties

1. Introduction

In the recent years, complex perovskites oxide ceramics are very promising for electronic applications. Many authors have shown considerable interest in the electrical properties of these compounds. For dielectric applications, high dielectric constant in system of $A(Fe_{0.5}B_{0.5})O_3$ (A=Ba, Sr and B=Sb, Nb, Ta) has been extensively investigated by many authors [1–3]. $BaFe_{0.5}Nb_{0.5}O_3$(BFN) is an example of such materials which exhibits giant dielectric constant ($\varepsilon_r \approx 10^4$–$10^5$) over a wide temperature range [4]. The disorder in B-site cations in perovskite unit lattice was related to the high relative permittivity over a wide range of temperatures [5]. Diffused-phase transitions have also been observed in this material. The dielectric properties of BFN have been related to the electrical characteristic at the grain boundary region [5,6]. Improvements of dielectric properties have been found for modified BFN such as La doped BFN [4].

Previous work by Raevski et al. reported that $Sr(Fe_{0.5}Nb_{0.5})O_3$(SFN) is an interesting $A(Fe_{0.5}B_{0.5})O_3$ compound due to its high dielectric constant. Many properties of SFN have been studied and reported. Saha and Sinha reported that SFN showed a monoclinic crystal symmetry [7] while Liu et al. reported it as an orthorhombic symmetry [8]. Saha and Sinha investigated the dielectric characteristics over wide frequency and temperature ranges and the dielectric constant of SFN were $\sim 10^3$–10^4. This material also exhibits a dielectric relaxation behavior which is similar to BFN [2]. The dielectric behavior of $Sr(Fe_{0.5}Nb_{0.5})O_3$ ceramics has been interpreted on the basis of the Maxwell-Wagner mechanism [7,9]. Magnetic properties of SFN were investigated by Tezuka et al. [10]. Although the properties of SFN are interesting, the effects of doping on properties of SFN have not been widely investigated. In the present work, we report our investigation on the properties of SFN ceramics doped with Ho for the first time. The modified SFN samples were synthesized via a solid-state reaction.

2. Experimental

In the present work, $Sr(Fe_{1-x}Ho_x)_{0.5}Nb_{0.5}O_3$ (SFHN) was synthesized via solid-state reaction of $SrCO_3$(Aldrich, 99.0% purity), Fe_2O_3(Aldrich, 99.0% purity) and Ho_2O_3(Aldrich, 99.9% purity) and Nb_2O_5(Aldrich, 99.9% purity). The raw materials were weighed to give the desired composition, and

*Corresponding author at: Department of Physics and Materials Science, Faculty of Science, Chiang Mai University, Chiang Mai 50200, Thailand. Tel.: +66 53 943376; fax: +66 53 357512.
E-mail address: rujijanagul@yahoo.com (G. Rujijanagul).

0272-8842/$ - see front matter © 2012 Elsevier Ltd and Techna Group S.r.l. All rights reserved.
http://dx.doi.org/10.1016/j.ceramint.2012.10.067

then suspended in ethanol and intimately mixed in a ball milling machine for 24 h using zirconia as a grinding media. After drying for 24 h, the powder was ground, sieved and then calcined at 1100–1300 °C for 3 h with a heating/cooling rate 5 °C/min. The obtained mixture was dried and uniaxially pressed into a disc shape. The green discs were sintered in air at 1400–1500 °C with a dwell time of 3 h and a heating/cooling rate of 5 °C/min. The density of the sintered samples was determined by Archimedes' principle. Phase formation in the samples was determined by X-ray diffraction (XRD). For electrical measurement, the sintered samples were polished to obtain parallel surfaces and silver paste electrodes were applied to make an electrode. The dielectric properties of the pellet ceramics were measured using a LCR meter.

3. Results and discussion

The XRD patterns of pure and modified SFN ceramics are shown in Fig. 1. The XRD result shows that all diffraction peaks of the undoped sample correspond to an orthorhombic perovskite phase according to JCPDS file no. 01-070-5965. The result agrees with the work done by Lui et al [8]. With increasing Ho concentration, however, all diffraction peaks shifted to lower angles. Further at high angles of the diffraction patterns ($2\theta \sim 75$–77°), three main peaks ((332), (240), and (116) reflections) transformed to a single broad main peak, indicating that the orthorhombic phase transformed to a pseudocubic phase. An extra impurity peak was observed at 2–32° for the $x=0.15$ sample (index by ⁎). The impurity phase was identified as Ho_2O_3 according to JCPDS file no. 00-019-0554. In the present work, it is possible that partial Ho^{3+} ions substituted Fe^{3+} ions in the lattices as a result in the phase transformation. For the higher doped samples, however, it is believed that most of the holmium oxide compound segregated and presented especially at the grain boundary, due to the small solubility limit of Ho in SFN.

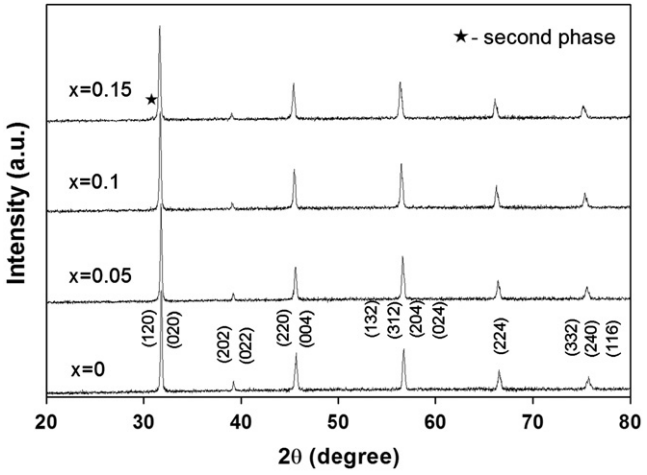

Fig. 1. X-ray diffraction patterns of Ho_2O_3 doped SFN ceramics.

The dielectric constant and dielectric loss as a function of frequency is shown in Fig. 2. The dielectric constant of all samples exhibited a frequency dependent. The samples also showed higher dielectric constants at lower frequencies. This can be attributed to the presence of all different types of polarizations, i.e. interfacial, dipolar, atomic, ionic, electronic contribution in the material. However, the dielectric constant of the samples decreased with increasing frequency due to some polarizations as mentioned above may have less contribution [11]. The dielectric loss result shows a frequency

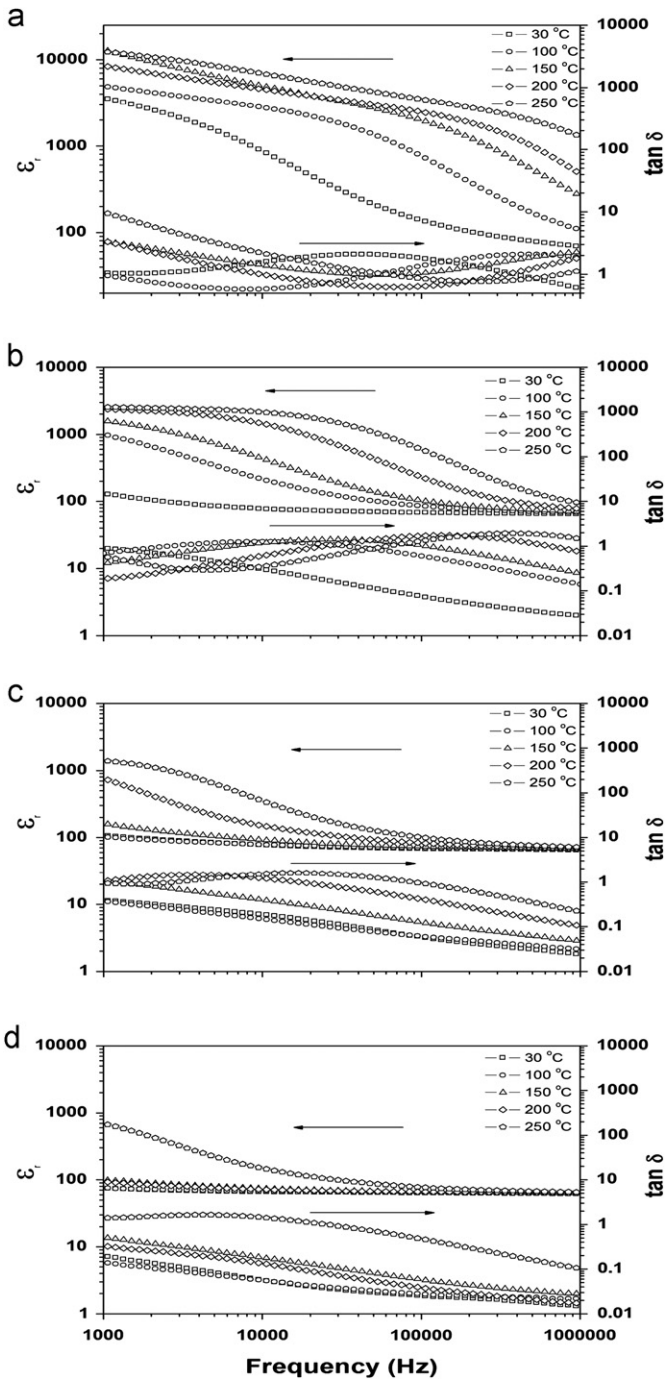

Fig. 2. Frequency dependence of dielectric constant and dielectric loss for SFHN ceramics: (a) $x=0$; (b) $x=0.05$; (c) $x=0.10$ and (d) $x=0.15$.

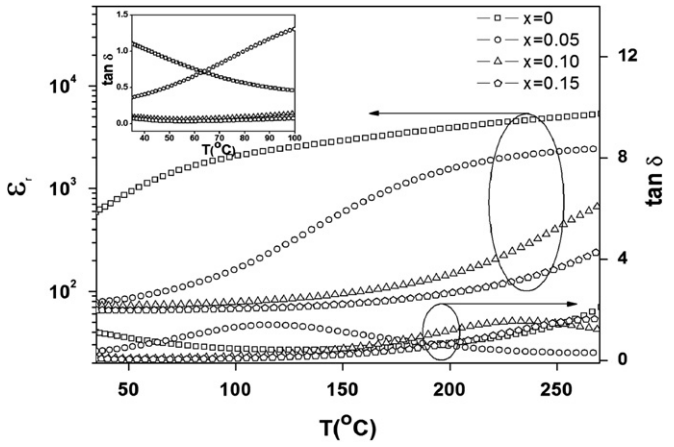

Fig. 3. Dielectric constant and dielectric loss versus temperature for undoped and doped SFN ceramics.

dependence, due to the non-constant concentration of charge carriers [11]. In addition, the dielectric loss decreased with increasing Ho concentration especially at high frequencies. The reduction of tangent loss may be related to the changes in the transport behavior that contributed to a higher resistance [12].

The temperature dependence of the dielectric properties for the undoped SFN and doped SFN ceramics at 10 kHz is shown in Fig. 3. For undoped SFN, the dielectric constant increased with temperature and the dielectric loss–temperature curve showed a wide plateau region with high dielectric constants for temperature above ~75 °C (extrapolated from onset temperature of the curve). The dielectric–temperature behavior and dielectric maximum for the unmodified SFN are similar to that observed in previous work [7]. In doped samples, Ho doping shifted the high dielectric constant region to higher temperatures and suppressed dielectric constant. This behavior can be found in Sr doped $CaCu_3Ti_4O_{12}$ (CCTO), reported by Li et al. [13]. However, the dielectric loss reduced with increasing Ho concentration (from room temperature to 100 °C), inset (b) of Fig. 3. The high dielectric constant in SFN ceramic may be due to the presence of Fe^{2+} in sintered SFN ceramics, as proposed by Ananta and Thomas [14], and co-existence of Fe^{2+} and Fe^{3+} ions can give rise to Fe^{3+}–Fe^{2+} ions polaron hopping conduction mechanism. In doped ceramics, the substitution of Ho^{3+} ions to B-site (Fe^{3+} ions) in the lattices can reduce Fe^{3+}–Fe^{2+} ions. This may limit the polaron hopping conduction; resulting in the suppression of dielectric constant and increase the resistivity [15,16]. The doping also produced a shift in temperature at dielectric loss maximum to higher temperature. In addition, the dielectric loss–temperature curve of each ceramic exhibited a dielectric relaxation behavior (not shown there).

Variation of the relaxation temperature with frequency was fitted via the following expression:

$$f = f_0 \exp\left(-\frac{E_a}{kT}\right) \quad (1)$$

where f_0 is the pre-exponential term, E_a is the activation energy, and k is Boltzmann's constant. It was found that the Ho doping resulted in a significant change in activation energy values. Values of E_a as calculated from Eq. (1) were 0.33, 0.47, 0.74 and 0.81 eV for $x=0.00$, 0.05, 0.10 and 0.15 samples, respectively. The E_a value of 0.33 eV for the undoped SFN is closed to the value obtained by Liu et al. (0.38 eV) [8]. Further, the increase in E_a value with doping concentration is similar to the work done by Wu et al. in $Y_3Fe_{5-x}Ti_xO_{12+x/2}$ ceramics [17].

The dielectric behavior of the studied ceramics can be further analyzed with the impedance spectroscopy technique. Fig. 4 shows complex impedance plane measured at room temperature and 250 °C.

Generally, many polycrystalline materials show two semicircles where the high-frequency arc associates with the electrical behavior of grain (bulk grain) and the low-frequency arc represents the electrical behavior due to the grain boundary behavior. Data collected from the plot can be analyzed by an equivalent circuit of one parallel resistance–capacitance (RC) element or other equivalent

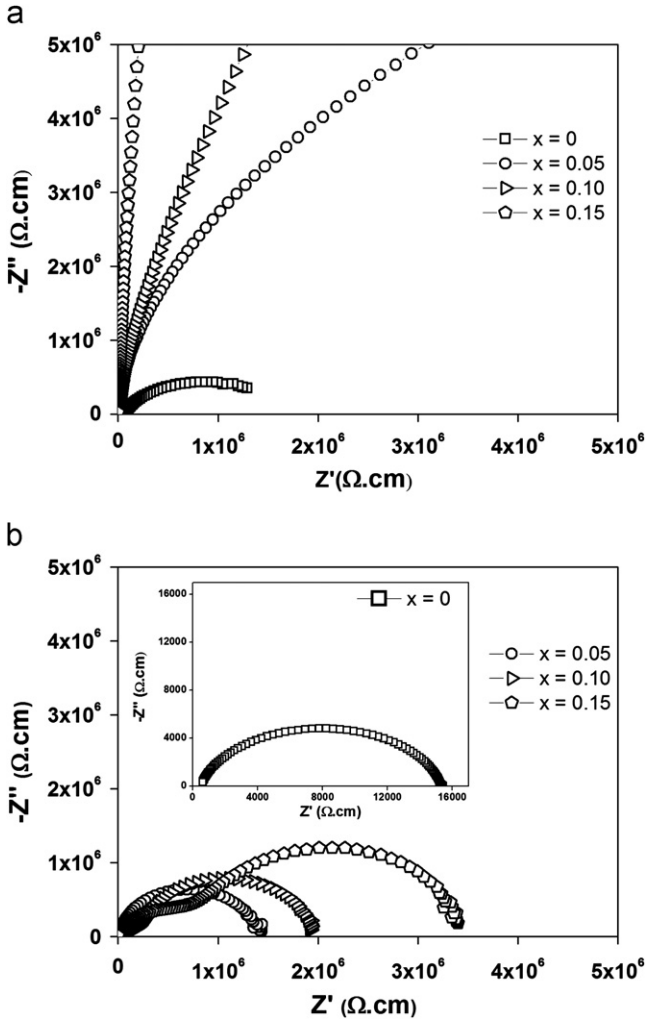

Fig. 4. Complex impedance spectrums of SFHN ceramics at (a) room temperature and (b) 250 °C.

circuits. Based on the work done by Li et al. [18], resistance of grain (R_g) and grain boundary (R_{gb}) can be determined by using the two equivalent parallel circuits, giving rise to two arcs in the complex plane. In the present work at room temperature, diameter of the arcs at lower-frequency is comparably bigger than diameters of the arcs at high-frequency. This result indicates that the value of R_{gb} associated with the big arc is much larger than that of the small arc. Therefore, resistance in the equivalent circuit is dominated by grain boundary. Further, diameter of the big arc increased with increasing Ho concentration, implying that the Ho doping produced an increase in resistance of the grain boundary. This result indicates that Ho doping influenced the impedance characteristic, especially for the grain boundary at room temperature.

Curve fittings of the impedance data were performed and the values of R_g and R_{gb} were estimated, as shown in Fig. 5. General trend shows that values of R_g and R_{gb} increased with Ho concentration. However, the rapid increase in R_{gb} at room temperature with Ho concentration indicated a strong effect of the doping on the grain boundary characteristic. This result matches the trend of dielectric loss where dielectric loss has a tendency to decrease with increasing Ho concentration (near room temperature). At the high temperature (250 °C), the doping had a stronger effect on R_g rather than R_{gb}, where R_g increased with higher rate (with Ho concentration) than R_{gb}. This may be due to the intrinsic properties of SFHN (lattice characteristic).

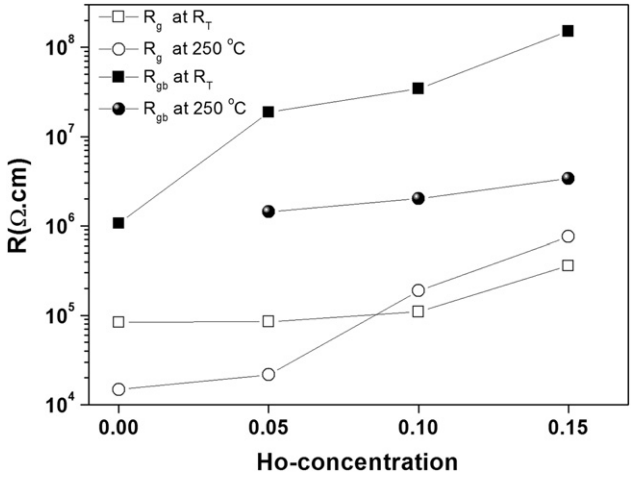

Fig. 5. Values of R_{gb} and R_g versus Ho concentration at room temperature and 250 °C.

The frequency dependence of electric modulus (M'') at room temperature and 250 °C are displayed in Fig. 6. In general, the response frequencies of grain boundaries and grains fall into two different frequency regions, i.e. the higher frequency responses can be attributed to the contribution from the grain characteristic while the lower frequency responses can be linked to the grain boundaries characteristic. In the present work, the log M'' spectrum of the undoped sample at room temperature showed a peak at a high frequency. The peak of log M'' shifted to a lower frequency for the $x=0.05$ sample and became a plateau for the $x=0.10$ sample. In case the $x=0.15$ sample, it seems that the plateau showed two peaks where the higher peak occurred at a low frequency and the lower peak occurred at a high frequency. This result indicates the domination of the grain boundary for higher Ho concentration samples. At the high temperature (250 °C), it seems that log M'' spectrum of the undoped sample showed two peaks. However, the two peaks had a tendency to become a single peak for higher Ho concentrations. This result indicates that grain characteristic had contributed to the electrical properties of the samples at high temperature. Further, the single peaks (at room temperature) became two peaks at high temperature, indicating that grain boundary characteristic was changed by temperature. These results are consistent with that obtain from the complex impedance plots.

4. Conclusion

Effects of Ho doping on the dielectric properties of strontium iron niobate (SFN) ceramics were investigated for the first time. The orthorhombic phase as observed in SFN transform to the pseudocubic phase for higher Ho concentrations. However, the low solubility limit of Ho in SFN resulted in a formation of the impurity phase for the $x=0.15$ ceramic. The doping promoted a reduction in dielectric loss due to the increase in grain boundary

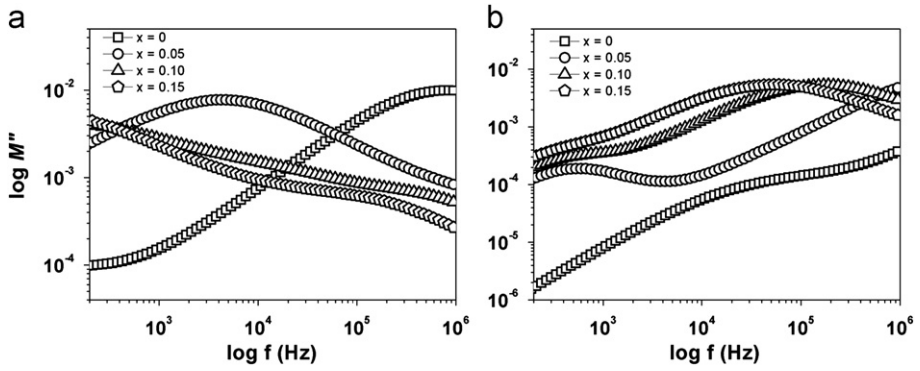

Fig. 6. Frequency dependence of log $M''$of SFHN ceramics at (a) room temperature and (b) 250 °C.

resistance. The change in dielectric constant with Ho concentration was linked to the Fe^{3+}–Fe^{2+} ions polaron hopping mechanism. However, further investigation should be performed to confirm the reason.

Acknowledgments

This work was supported by the National Research University (NRU), the Office of Higher Education Commission (OHEC), Thailand center of excellence in Physics (Thep) and Faculty of Science and Graduate School Chiang Mai University.

References

[1] S. Ming Ke, H. Fan, H. Tao Huang, Dielectric relaxation in A_2FeNbO_6 (A = Ba, Sr, and Ca) perovskite ceramics, Journal of Electroceramics 22 (2009) 252–256.

[2] S. Saha, T.P. Sinha, Structural and dielectric studies of $BaFe_{0.5}Nb_{0.5}O_3$, Journal of Physics: Condensed Matter 14 (2002) 249–258.

[3] Z. Wang, X.M. Chen, L. Ni, Y.Y. Liu, X.Q. Liu, Dielectric relaxations in $Ba(Fe_{1/2}Ta_{1/2})O_3$ giant dielectric constant ceramics, Applied Physics Letters 90 (2007) 102905.

[4] C. Chao-Yu, C. Yen-Hwei, C. Guo-Ju, Effects of lanthanum doping on the dielectric properties of $Ba(Fe_{0.5}Nb_{0.5})O_3$ ceramic, Journal of Applied Physics 96 (2004) 6624.

[5] C. Chao-Yu, C. Yee-Shin, C. Guo-Ju, C. Ching-Chang, H. Tzu-Wei, Effects of bismuth doping on the dielectric properties of $Ba(Fe_{0.5}Nb_{0.5})O_3$ ceramic, Solid State communication 145 (2008) 212–217.

[6] M. Yokosuka, Dielectric dispersion of the complex perovskite oxide $Ba(Fe_{1/2}Nb_{0.5})O_3$ at low frequencies, Japanese Journal of Applied Physics 34 (1995) 5338.

[7] S. Saha, T.P. Sinha, Dielectric relaxation in $SrFe_{1/2}Nb_{1/2}O_3$, Journal of Applied Physics 99 (2006) 014109.

[8] Y.Y. Liu, X.M. Chen, X.Q. Liu, L. Li, Giant dielectric response and relaxor behaviors induced by charge and defect ordering in $SrFe_{1/2}Nb_{1/2}O_3$ ceramics, Applied Physics Letters 90 (2007) 192905.

[9] I.P. Raevski, S.A. Prosandeev, A.S. Bogatin, M.A. Malitskaya, L. Jastrabik, High dielectric permittivity in $AFe_{1/2}B_{1/2}O_3$ nonferroelectric perovskite ceramics (A = Ba, Sr, Ca; B = Nb, Ta, Sb), Journal of Applied Physics 93 (2003) 4130.

[10] K. Tezuka, K. Henmi, Y. Hinatsu, N.M. Masaki, Magnetic susceptibilities and mössbauer spectra of perovskites A_2FeNbO_6 (A = Sr, Ba), Journal of Solid State Chemistry 154 (2000) 591–597.

[11] U. Intatha, S. Eitssayeam, J. Wang, T. Tunkasiri, Impedance study of giant dielectric permittivity in $BaFe_{0.5}Nb_{0.5}O_3$ perovskite ceramic, Current Applied Physics 10 (2010) 21–25.

[12] S. Kwon, C.C. Huang, E.A. Patterson, D.P. Cann, E.F. Alberta, S. Kwon, W.S. Hackenberger, D.P. Cann, The effect of Cr_2O_3, Nb_2O_5 and ZrO_2 doping on the dielectric properties of $CaCu_3Ti_4O_{12}$, Materials Letters 62 (2008) 633–636.

[13] W. Li, R.W. Schwartz, A. Chen, J. Zhu, Dielectric response of Sr doped $CaCu_3Ti_4O_{12}$ ceramics, Applied Physics Letters 90 (2007) 112901.

[14] S. Ananta, N.W. Thomas, Relationships between sintering conditions, microstructure and dielectric properties of lead iron niobate, Journal of the European Ceramic Society 19 (1999) 1873–1881.

[15] S. Bhukal, T. Namgyal, S. Mor, S. Bansal, S. Singhal, Structural, electrical, optical and magnetic properties of chromium substituted Co–Zn nanoferrites $Co_{0.6}Zn_{0.4}Cr_xFe_{2-x}O_4$ ($0 \le x \le 1.0$) prepared via sol–gel auto-combustion method, Journal of Molecular Structure 1012 (2012) 162–167.

[16] M.A. Gabal, Y.M. Al Angari, Effect of chromium ion substitution on the electromagnetic properties of nickel ferrite, Materials Chemistry and Physics 118 (2009) 153–160.

[17] Y.J. Wu, C. Yu, X.M. Chen, J. Li, Magnetodielectric effects of $Y_3Fe_{5-x}Ti_xO_{12+x/2}$ ceramics, Applied Physics Letters 100 (2012) 052902.

[18] M. Li, A. Feteira, D.C. Sinclair, Origin of the high permittivity in $(La_{0.4}Ba_{0.4}Ca_{0.2})(Mn_{0.4}Ti_{0.6})O_3$ ceramics, Journal of Applied Physics 98 (2005) 084101.